Journal of Photochemistry and Photobiology A: Chemistry 207 (2009) 244–253

Contents lists available at ScienceDirect

Journal of Photochemistry and Photobiology A: Chemistry

journal homepage: www.elsevier.com/locate/jphotochem

Enhanced photocatalytic activity under visible light in N-doped TiO_2 thin films produced by APCVD preparations using t-butylamine as a nitrogen source and their potential for antibacterial films

Charles W.H. Dunnill[a], Zoie A. Aiken[b], Jonathan Pratten[b], Michael Wilson[b], David J. Morgan[c], Ivan P. Parkin[a,*]

[a] Centre for Materials Research, Department of Chemistry, University College London, 20 Gordon Street, London WC1H 0AJ, UK
[b] UCL Eastman Dental Institute, University College London, 256 Gray's Inn Road, London WC1X 8LD, UK
[c] Cardiff Catalysis Institute, School of Chemistry, Cardiff University, Main Building, Park Place, Cardiff CF10 3AT, UK

ARTICLE INFO

Article history:
Received 22 May 2009
Received in revised form 15 July 2009
Accepted 17 July 2009
Available online 5 August 2009

Keywords:
Photocatalysis
N-TiO_2
Visible light

ABSTRACT

Atmospheric pressure chemical vapour deposition (APCVD) of N-doped titania thin films has been achieved from titanium (IV) chloride, ethyl acetate and t-butylamine at a deposition temperature of 500 °C and the films characterised by XRD, Raman spectroscopy, XPS, SEM, UV–visible–NIR spectroscopy, contact angle measurements and stearic acid degradation. The films were compared to two industrial self-cleaning products: Activ™ and BIOCLEAN™ and shown to be significantly better in both photocatalysis and superhydrophilicity, two preferential properties of effective self-cleaning coatings. X-ray diffraction showed the films have the anatase TiO_2 structure. High resolution X-ray photoelectron spectroscopy was consistent with small quantities of nitrogen (0.15–0.7 at.%) occupying an interstitial site (N 1s ionisation at ~400 eV). This work sheds light on the current confusion within the literature as to the role of nitrogen in the enhancement of the photocatalytic properties of thin films with direct evidence that selective doping at the interstitial site (ionisation ~400 eV by XPS) has a pronounced effect on enhancing photocatalysis. Surprisingly in the majority of films no XPS peak for N for O substitution was observed (ionisation ~396 eV by XPS). This is to our knowledge the first example of an N-doped titania film with only interstitial doping. These films showed significant photocatalysis with visible light. The best films were tested for their antimicrobial properties and found to be an effective agent for the destruction of *Escherichia coli* using lighting conditions commonly found in UK hospitals.

1. Introduction

Titanium dioxide (TiO_2) films were first commercialised worldwide for self-cleaning window glass in 2002 with the launch of Pilkington Activ™ glass [1]. These coatings have been considered one of the most important advances in glass technology for many decades [2], and have also been commercialised by other glass companies such as Saint Goban (BIOCLEAN™) [3] and PPG (Sunclean) [4]. Self-cleaning coatings work by the photocatalytic destruction of organic pollutants, and the engendered superhydrophilicity [5]. These factors enable dirt to be loosened and photomineralised by the photoactivity and then to be washed off uniformly by rainwater that sheets on the surface. While highly successful, commercialised and widely sold (>1×10^6 m^2 Pa), there is interest in improving the activity and application of these TiO_2 coatings as well as adapting the current technology to other areas such as antibacterial applications [6,7]. One such approach is to shift the band onset from UV into the visible region of the spectrum as 98% of photons from solar energy have wavelengths >385 nm [8]. The vast increase in number of available photons with which to perform the photocatalysis, even by a small shift (10's of nm) of the band onset into the visible should improve the photocatalytic properties of the film, while retaining the other useful properties such as hardness, ease of production, adhesion to the glass surface and superhydrophilicity. Furthermore, the availability of a visible light-driven photocatalyst with self-cleaning properties unveils a plethora of potential applications where there is a ready supply of white light and little UV, such as interior household and hospital locations especially hand-touch surfaces susceptible to bacterial transfer [6].

Organisms such as *Escherichia coli* and other *Enterobacteriaceae* are found in the large intestine and are used as indicators of faecal contamination when testing food and food surfaces [9]. This organism is often observed on toilet flush handles, door handles, taps and other areas that are frequently touched by unwashed hands. These,

* Corresponding author. Tel.: +44 207 679 4669.
E-mail address: I.P.Parkin@ucl.ac.uk (I.P. Parkin).

1010-6030/$ – see front matter © 2009 Elsevier B.V. All rights reserved.
doi:10.1016/j.jphotochem.2009.07.024

amongst other areas, harbour bacteria and can act as reservoirs for infection, contributing towards the spread of healthcare-associated infection. Healthcare-associated infections are an increasing problem with an estimated 100,000 deaths in the United States during 2002 [10].

It has been shown that Gram-negative organisms are less susceptible to killing by light-activated antimicrobial coatings than Gram-positive organisms such as *Staphylococcus aureus* [11]. If an antimicrobial coating were effective against Gram-negative organisms, such as *E. coli*, it would serve as a good marker for antimicrobial action against other organisms such as methicillin-resistant *S. aureus* (MRSA).

Much work has been carried out in attempting to shift the band gap of TiO_2 by nitrogen doping to form N-doped TiO_2 films [12–25]. Many methods have been employed, including reactions with ammonia [13,19–21], hydrazine [14], nitrogen dioxide [12], pulsed laser deposition [17] and a nitrogen plasma or ion bombardment/spluttering [13,15,16,22–25]. Somewhat contradictory results have been obtained when compared to pure TiO_2 [26]. The incorporation of nitrogen into the TiO_2 structure can take many forms with oxygen replacement, i.e. the formation of $TiO_{2-x}N_x$, or the formation of TiO_2N_x ($x < 3$ at.%) with interstitial nitrogen. To date to the best of our knowledge, no thin film of N-doped titania has been formed in which the nitrogen is solely located in an interstitial site, though Peng et al. do show that while both interstitial and substitutional doping does enhance the photocatalytic effects with interstitial being more pronounced [27]. Low concentrations of nitrogen dopants are also seen to be favourable [17].

Here we report the production of a series of visible light-driven photocatalytic films produced utilizing a simple methodology involving the APCVD of titanium (IV) chloride, ethyl acetate and t-butylamine at 500 °C and is consistent with technology and techniques currently employed in the float glass industry, e.g. Activ™ glass is currently prepared using titanium (IV) chloride and ethyl acetate. The system has been investigated both for the trends associated with nitrogen content and with the deposition time. Our initial findings indicated that control of nitrogen content was possible by controlling the mass flow of the amine precursor via the temperature of the amine reservoir. The series of films produced have been compared to two of the current industry leading products for self-cleaning glass: Pilkington Activ™ and Saint-Gobain BIOCLEAN™. We show that the N-doped films are effective photocatalysis, especially with interstitial nitrogen dopants and that they are effective in killing *E. coli* with visible light. This work constitutes the first study of N-doped titania thin films to kill bacteria. It also shows that the 400 eV XPS ionisation associated with N-interstitial doping is vital for the visible light photoactivity and than N-doped films in which the nitrogen is only present in a interstitial position can be conveniently made using t-butylamine as the nitrogen source.

2. Methods

CVD preparations were carried out using a custom built, horizontal, cold walled APCVD quartz deposition chamber. The deposition chamber consisted of a quartz tube of ~100 mm diameter and 360 mm length and contained a graphite reactor bed with three cartridge heaters (Whatman) on which the glass substrates were positioned. A steel sheet was used to limit the volume of the reactor, giving the reacting gasses approximately 7 mm of space above the glass substrate, as shown in Fig. 1.

Nitrogen gas (BOC 99%) supplied from a cylinder was used as the carrier gas and was preheated, bubbled through the reservoirs and passed into the heated mixing chambers prior to reaching the glass substrate in the deposition chamber. At each stage the temperature and flow of the nitrogen was independently controllable.

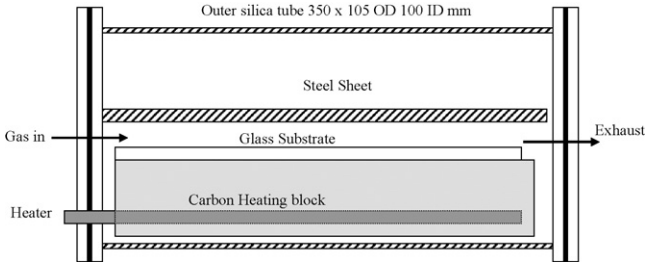

Fig. 1. Schematic of the horizontal cold walled APCVD quartz reactor used in these preparations.

The depositions were carried out on the SiO_2 surface of slides of standard float glass from Pilkington [1] of dimensions 220 mm × 85 mm × 4 mm (length × width × thickness) coated on one side with a barrier layer of SiO_2 to prevent ion diffusion from the glass to the film. The glass was washed prior to insertion into the APCVD reactor using sequential washings of water, acetone, petroleum ether (60–80) and propan-2-ol giving a clean and smear free finish.

In all preparations discussed the glass substrates were heated at 10 °C min^{-1} from room temperature to 500 °C and allowed to equilibrate for >45 min, prior to the deposition reactions. The precursors used were titanium (IV) chloride (Aldrich) as the titanium source, ethyl acetate (BOC 99.0%) as the oxygen source and t-butylamine (Fisher scientific 99.5%) as the nitrogen source. The nitrogen carrier gas for the titanium (IV) chloride and ethyl acetate was preheated to ~150 °C with a flow rate of 0.5 l min^{-1}. The bubblers were heated to 70 and 40 °C respectively to give a molar mass flow ratio of 1:2. These reactants were premixed in a single mixing chamber at 250 °C with an additional flow of 6 l min^{-1} carrier gas preheated to 150 °C. The nitrogen doping was achieved using a preheated carrier gas at 60 °C flowing at 0.1 l min^{-1} through the t-butylamine reservoir whose temperature was controlled using a water bath containing 50:50 H_2O:ethylene glycol (0–15 °C). The t-butylamine was introduced to the titanium (IV) chloride and ethyl acetate mixture just before contact with the glass substrate at a temperature of 100 °C and an additional flow of 1 l min^{-1}, as shown in the schematic in Fig. 2.

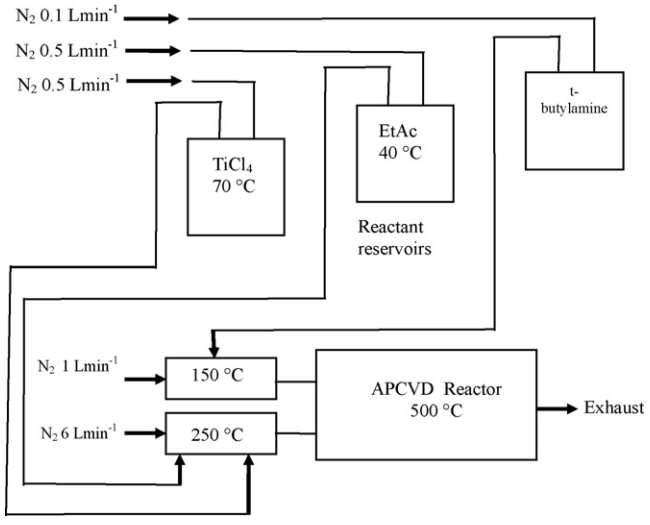

Fig. 2. Schematic of the gas lines and reactant reservoirs used in the preparations discussed. The temperature and flow rate of the titanium (IV) chloride and ethyl acetate reservoirs leads to a ratio of ~1:2.5 $TiCl_4$:EtAc which is desirable for the growth of anatase films under the conditions of the reactor.

Table 1
The sample names and the experimental conditions for the thin films of N-doped TiO_2 formed from the APCVD of titanium (IV) chloride, ethyl acetate and t-butylamine at 500 °C. The sample names are those used in the figures with the relative information given in the legends. Samples **A** and **B** refer to the two industry standards Activ™ and BIOCLEAN™ respectively.

Sample	Temperature of t-butylamine reservoir (°C)	Molar mass flow of t-butylamine (mmol min^{-1})	Approx. mass flow ratios, $TiCl_4$:EtAc:t-butylamine	Deposition time (s)
A		Commercial product Activ™		
B		Commercial product BIOCLEAN™		
C	0	0.7	1:2.5:0.2	30
D	5	1	1:2.5:0.3	30
E	10	1.4	1:2.5:0.5	30
F	15	1.9	1:2.5:0.6	30
G	5	1	1:2.5:0.3	60
H	5	1	1:2.5:0.3	120

In this series of experiments both the temperature of the t-butylamine reservoir and the deposition time were varied. The mass flow rate of the t-butylamine was calculated from the volatility data for t-butylamine and is given in Table 1 which also shows the sample preparation conditions used in the films discussed in this paper along with the referencing sequences used throughout this work.

X-ray diffraction was achieved using a Bruker-Axs D8 (GADDS) diffractometer, utilizing a large 2D area detector and a Cu X-ray source, monochromated (Kα1 and Kα2) fitted with a Gobble mirror. The instrumental setup allowed 34° in both θ and ω with a 0.01° resolution and 3–4 mm^2 of sample surface illuminated at any one time. Multiple Debye–Scherrer cones were recorded simultaneously by the area detector with two sections covering the 65° 2θ range. The Debye–Scherrer cones, once collected were integrated along ω to produce standard 1D diffraction patterns of degrees 2θ against intensity. Scan data were collected for 800 s periods to give sufficiently resolved peaks for indexing. Raman was achieved using a Renishaw in Via Raman microscope, and UV–visible–NIR; transmission and reflectance measurements were achieved using a PerkinElmer λ950. Scanning electron microscopy was performed using secondary electron imaging on a JEOL 6301 field emission instrument. High resolution X-ray photoelectron spectroscopy (XPS) was performed at Cardiff University on a Kratos Axis Ultra-DLD photoelectron spectrometer using monochromatic Al-K_α radiation. Survey spectra were collected at a pass energy of 160 eV, while narrow scans acquired at a pass energy of 40 eV, charge neutralization of the samples was achieved using the Kratos immersion lens neutralization system. The data were analysed using CasaXPS™ software and calibrated to the C (1s) signal at 284.7 eV, attributed to adventitious carbon. Scanning electron microscopy was achieved using secondary electron imaging on a JEOL 6301 field emission instrument.

The photocatalytic activity of the films was quantified using the destruction of stearic acid. There are many issues with the use of stearic acid as a measurement of photocatalytic activity of thin films, one of which is the questionable comparability between results taken using different methods. It remains however, the benchmark of photocatalytic assessment for thin films. Much time has been spent refining the methodology to achieve the optimum conditions for a reproducible and representative test. While some methods differ significantly the majority involve applying the stearic acid to the surface and monitoring its destruction using the IR peaks that correspond to the C–H stretches in the stearic acid molecules. Stearic acid absorbs at: 2958 cm^{-1} (C–H stretch CH_3), 2923 cm^{-1} (symmetric C–H stretch CH_2), and 2853 cm^{-1} (asymmetric C–H stretch CH_2). Generally the first peak, which is of low intensity, is ignored and the other two peaks integrated to give an approximate concentration of stearic acid on the surface. 1 cm^{-1} in integrated area corresponds to approximately 9.7×10^{15} molecules cm^{-2} [28]. The rate of decay can then be approximated and compared by normalising the concentration on stearic acid molecules on the surface as C/C_0 readings. Where C_0 is the initial concentration of stearic acid present and C is the concentration at any time.

The samples for photocatalytic testing were prepared in duplicate as sheets of ~30 mm × 30 mm with as uniform a thin film as possible. These sheets were irradiated in a light box under 254 nm radiation to ensure that the surfaces were clean and active and attached to an IR sample holder consisting of an aluminium sheet with a circular hole in its centre and stored in a clean dark draw for >72 h to ensure that the surfaces were no longer activated as a result of the UV irradiation. A 0.01 M solution of stearic acid in methanol was then applied drop-wise to the centre of the hole and allowed to evaporate, leaving the characteristic white smear. Drops of similar size and volume were estimated using a Pasteur pipette.

FTIR spectra were obtained between 2700 and 3000 cm^{-1} using a PerkinElmer Spectrum RX1 FTIR spectrometer, using a plain piece of glass as a background. C_x measurements were then taken at 24-h intervals as the sum of the integrated area of the two larger peaks resultant from the stearic acid (2885–2947 and 2830–2867 cm^{-1}) with the samples placed under a white light source in between measurements. Plots of normalised concentration of stearic acid on the surface (C_x/C_0) verses time were used to follow the destruction of stearic acid and hence the photocatalytic activity. The spectral power distribution chart for the light source (GE lighting 2D fluorescent GR10q-835 white, 28 W), which is in common use in hospitals and therefore relevant to the investigation is shown in Figs. 3 and 4. IR spectra for the films alone were taken and there was no peaks corresponding to the C–H stretches observed, indicating firstly that the entire integrated area of the peaks was due to the stearic acid and secondly that there was no carbon contamination in the films from the carbonatious precursors in the synthesis.

For the microbiology, *E. coli* ATCC 25922 was stored at −80 °C in 10% glycerol and maintained by weekly subculture onto 5% Columbia blood agar plates (Oxoid Ltd., Basingstoke, UK). A single colony was inoculated into 20 ml nutrient broth and incubated

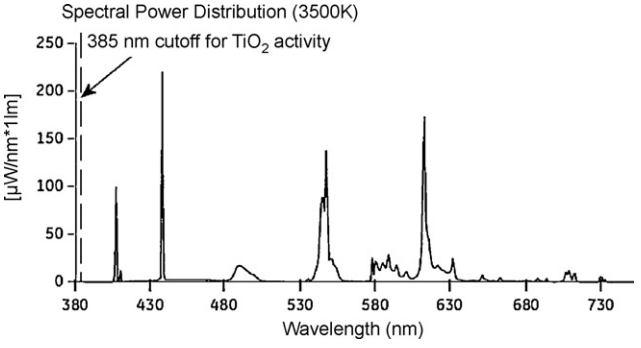

Fig. 3. Spectral power distribution diagram for the lamp used in the visible light photocatalysis measurements [48] marked with the cut-off for the activity of TiO_2, i.e. only photons of higher energy than 385 nm can activate TiO_2. The nearest emission line is at 410 nm. This light source is in common use in UK hospitals.

for 18 h at 37 °C in a rotating incubator (Sanyo BV, Loughborough, UK, 200 rpm). From the overnight culture, 1 ml was centrifuged at 12,000 rpm, and the pellet was re-suspended in 1 ml of phosphate-buffered saline. Approximately 300 μl of this suspension was added to 10 ml phosphate-buffered saline to achieve an optical density of 0.05 on a spectrophotometer at a wavelength of 600 nm (Pharmacia Biotech now GE Healthcare, Buckinghamshire, UK), which equates to approximately 10^7 cfu/ml. A 25 μl droplet was added to each coating occupying an area of 1 cm^2, so the final concentration was therefore 2.5×10^5 cfu/cm^2. The suspension was diluted and aliquoted onto MacConkey agar plates and aerobic colony counts calculated after 48 h incubation at 37 °C to estimate the bacterial load of the inoculum.

The film prepared with 1 mmol min^{-1} mass flow of t-butylamine and a 30 s deposition (sample **D**) was irradiated under a white light (General Electric 28 W Biax 2D compact fluorescent lamp) for 24 h, 20 cm from the light source, emitting an average light intensity of 5950 lx. After this incubation period, 25 μl of the prepared bacterial suspension (approximately 2.5×10^5 cfu/25 μl) was added to the coated sample before returning to the light source for a further 24 h. The light source was used as it is typically found in UK hospitals. The bacterial droplet was sampled for 20 s with a pre-moistened cotton-tipped swab, using a uniform, standardised method (the surface was sampled in three directions while rotating the head to ensure maximum absorbency) before re-suspending the swab in 1 ml phosphate-buffered saline. After a 2 min vortex, dilutions of 10^{-1}, 10^{-2} and 10^{-3} were plated out onto MacConkey plates, in duplicate and incubated for 48 h at 37 °C. Aerobic colony counts were determined and the results compared to the controls.

Two irradiation steps were used, one before the application of *E. coli* (A) and one after (L). The samples were either exposed to both irradiation steps (A+L+) or as controls, the first irradiation step and not the second (A+L−), the second irradiation step and not the first (A−L+) or incubated in the dark throughout, with no light exposure (A−L−). Two bacterial counts were produced for each exposure condition and the experimental procedure was performed in triplicate to demonstrate reproducibility.

The viable count data were subjected to statistical analysis using the Mann–Whitney in the SPSS program (version 16.0; SPSS Inc., Chicago, IL, USA) and the number of bacteria recovered from each of the four light exposure conditions was compared.

3. Results

3.1. Synthesis and characterisation

Samples have been named according to the synthetic conditions under which they were produced, as explained in the Experimental Section. A table of sample names is given in Table 1.

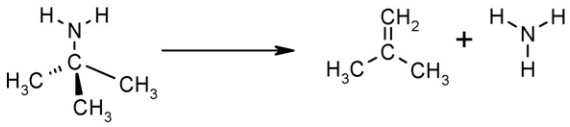

Fig. 4. Schematic of the *in situ* ammonia formation for the N-doping of TiO_2 films.

N-doped titania films were prepared by the APCVD reaction of titanium (IV) chloride, ethyl acetate and t-butylamine at a substrate temperature of 500 °C. Films were formed with different mass flow rates of t-butylamine, in order to vary the nitrogen content. The majority of films were formed with a deposition time of 30 s. The films appeared yellow in colour with uniform thickness. After synthesis, the samples were kept in the dark until ready for use. Prior to use the films were irradiated with 254 nm UV light to ensure that the surface was clean before testing and then stored in a clean dark drawer for >72 h to ensure that no activation from the irradiation was still present.

X-ray diffraction data (Fig. 5) of the films formed from the reaction of titanium (IV) chloride, ethyl acetate and t-butylamine by APCVD at 500 °C and with 30 s deposition times show peaks that match in position to those expected of anatase TiO_2. The crystallinity of the films and the resolution of the peaks are marginally reduced by the addition of nitrogen doping into the titania. The films were shown to be single-phase anatase except for the film formed with the lowest mass flow of t-butylamine which although essentially anatase showed tentative evidence for a minor amount of rutile. Surprisingly the film formed with a longer deposition time (sample **H**) shows predominantly rutile structure by XRD.

The films deposited over 30 s were shown to be anatase by Raman spectroscopy (Fig. 6) with no rutile phase present [29]. Sample **H** showed peaks for rutile structure as expected from the XRD data.

The films were analysed by high resolution XPS especially to show the nitrogen content and provide information on the position of N-doping. All films showed a nitrogen 1s ionisation at 400 eV which is indicative of interstitial nitrogen content [21,30–32]. The only sample to show an ionisation at 396 eV associated with O for N substitution was sample **E** which had a high mass flow of nitrogen and did so alongside a peak at 400 eV (Fig. 7).

Analysis of the XPS ionisation peak areas yielded atomic ratios of exactly 1:2 for the Ti:O indicating TiO_2 and suggesting interstitial doping rather than substitutional. The ratio of Ti:N was calculated from the relative peak areas and a trend observed that matched the molar flow of the t-butylamine used in the experiment. The

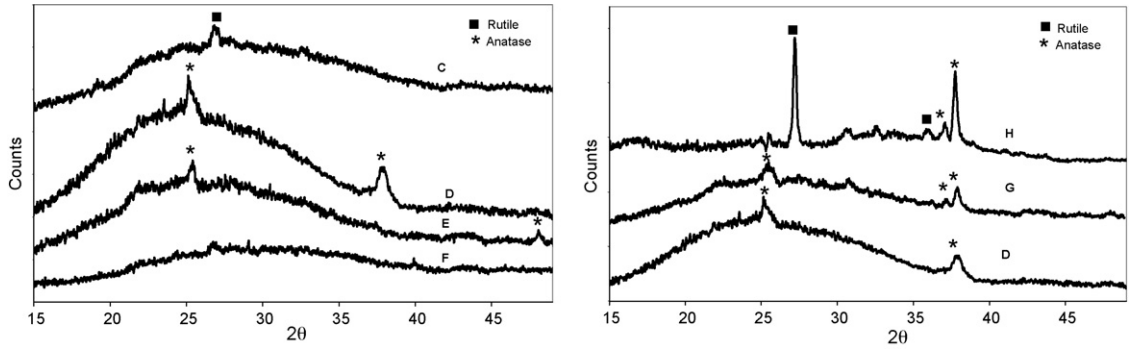

Fig. 5. XRD patterns for the thin films of N-doped TiO_2 formed from APCVD of titanium (IV) chloride, ethyl acetate and t-butylamine at 500 °C, showing the peaks that correspond to peak positions for anatase (*) and rutile (■) structures within the different N-doped TiO_2 films. Samples **C**, **D**, **E** and **F** were prepared with a molar mass flow of for the t-butylamine at 0.7, 1, 1.4 and 1.9 mmol min^{-1} respectively and 30 s deposition times while **G** and **H** were prepared with a 60 and 120 s deposition time respectively and a molar mass flow for the t-butylamine of 1 mmol min^{-1}.

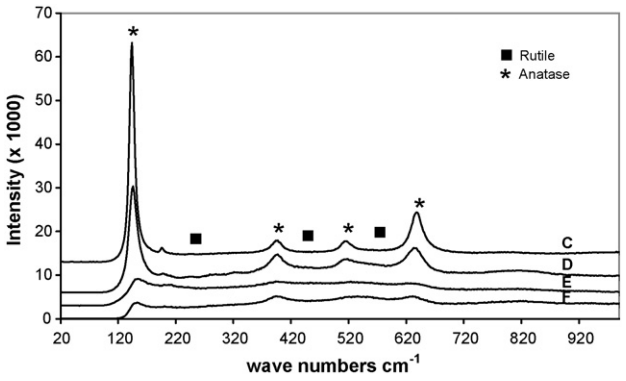

Fig. 6. Raman spectroscopy spectra of the thin films of N-doped TiO_2 formed from APCVD of titanium (IV) chloride, ethyl acetate and t-butylamine at 500 °C, showing no evidence for the rutile structure and a clear indication that the anatase structure of TiO_2 is present. Samples **C**, **D**, **E** and **F** were prepared with a molar mass flow of for the t-butylamine at 0.7, 1, 1.4 and 1.9 mmol min^{-1} respectively and 30 s deposition times.

range of values was from 0.15 to 0.7 at.% (Fig. 8). The quantification of the nitrogen content is below the detectable limits of some XPS spectrometers but within the range of the equipment at Cardiff. Sample **E** was not representative of the rest of the experiments as it showed an extra ionisation observed at 396 eV. This film also showed a low Ti:O ratio (ca. 1:1.8), again corresponding to the substitutional nature of the doping. Quite why the conditions used in the preparation of sample **E** should lead to substitutional doping as well as interstitial, while other samples only showed interstitial, is unclear, hence sample **E** appears to be an anomaly.

UV–visible–NIR spectra (Fig. 9) showed that the higher nitrogen content films had a deeper colour and slightly lower average transmission in the visible region of the spectrum (between 60 and 80%, 400–800 nm). All of the films had a transmission of 60% or better in the visible region, a key criterion for use in window glass. The samples were analysed for colour using $L^*a^*b^*$ coordinates in both transmission and reflection. L^* indicates lightness i.e. black (0) to white (100), a^* indicates green (−) to red (+) and b^* indicates blue (−) to yellow (+). All samples were light ($L^* > 88$), in the yellow region of the spectrum, as confirmed by the eye ($b^* = 0.25$ to 2.48) and showed variation in the green–red component ($a^* = -2.26$ to 4.07). There were more enhanced differences in the green–red component when comparing the transmission and reflection data for each individual sample ($a^* = -19.8$ to 4.9).

Reflectance spectra for the different films yield interference fringes allowing film thicknesses to be calculated using the Swanepoel method [33]. Samples **C**–**F** had thicknesses very close to 175 nm while **G** and **H** were thicker at 300 nm and 920 nm respectively. This equates to a growth rate of ~6 or 7 nm of film thickness per second.

The presence of nitrogen in the structure has an effect on the position of the band onset. A Tauc plot (Fig. 10(a)) was used to estimate the band onset of the semiconducting films and shows two groupings one grouping centred at 3.1 eV as would be expected for the films containing only TiO_2 and one grouping red shifted and spread closer to 2.8 eV.

The position of the band onset does not appear to depend on the quantity of nitrogen incorporation indicating that the while the nitrogen has a pronounced effect on the band onset it is not a simple matter of quantity. The furthest shifted is sample **D**, prepared with a mass flow of 1 mmol min^{-1} and a deposition time of 30 s, which coincides with the best visible light photocatalysis in the destruction of stearic acid (see below). Fig. 10(b) shows the variation in estimated band onset with the different deposition times. Both the 30 and 60 s depositions appear to have the

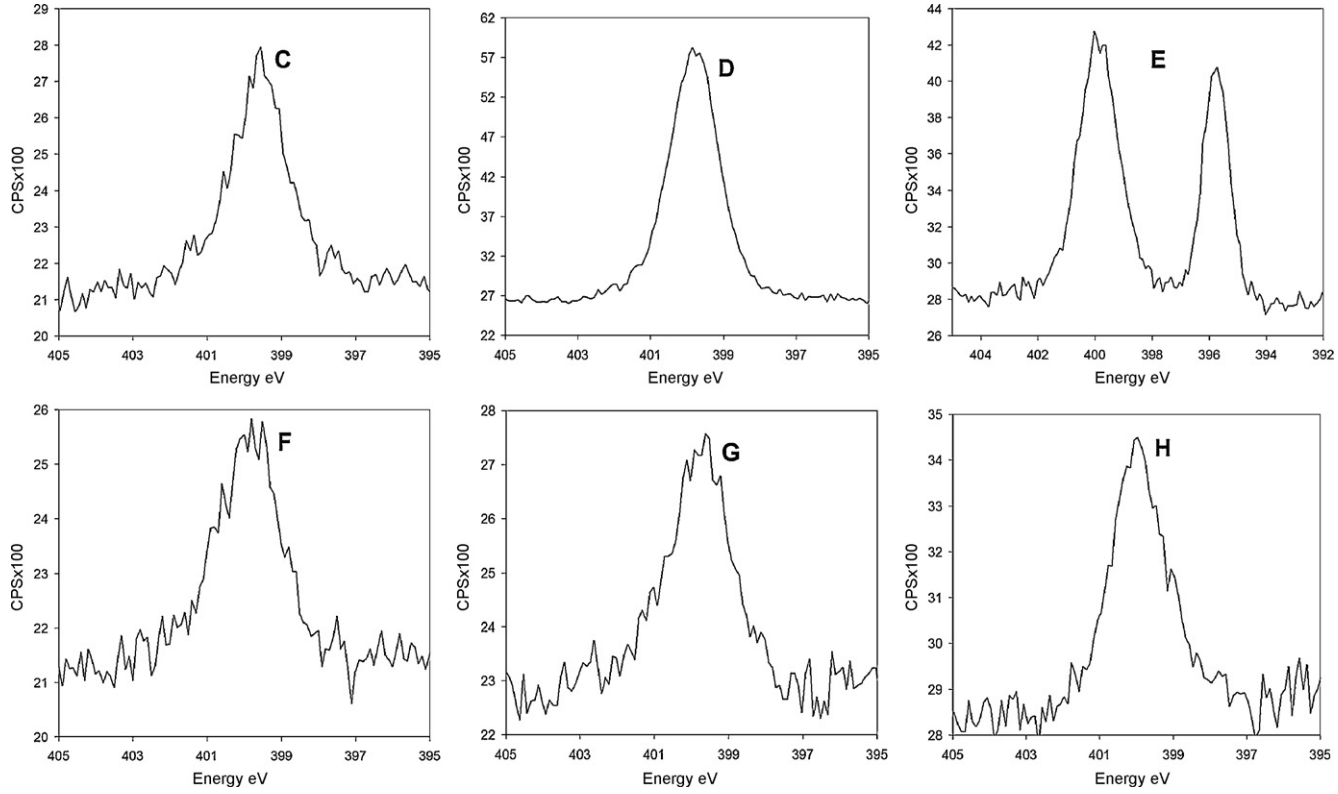

Fig. 7. XPS data showing the N 1s ionisations at 400 eV and at 396 eV for the thin films of N-doped TiO_2 formed from APCVD of titanium (IV) chloride, ethyl acetate and t-butylamine at 500 °C. Samples **C**, **D**, **E** and **F** were prepared with a molar mass flow of for the t-butylamine at 0.7, 1, 1.4 and 1.9 mmol min^{-1} respectively and 30 s deposition times while **G** and **H** were prepared with a 60 and 120 s deposition time respectively and a molar mass flow for the t-butylamine of 1 mmol min^{-1}.

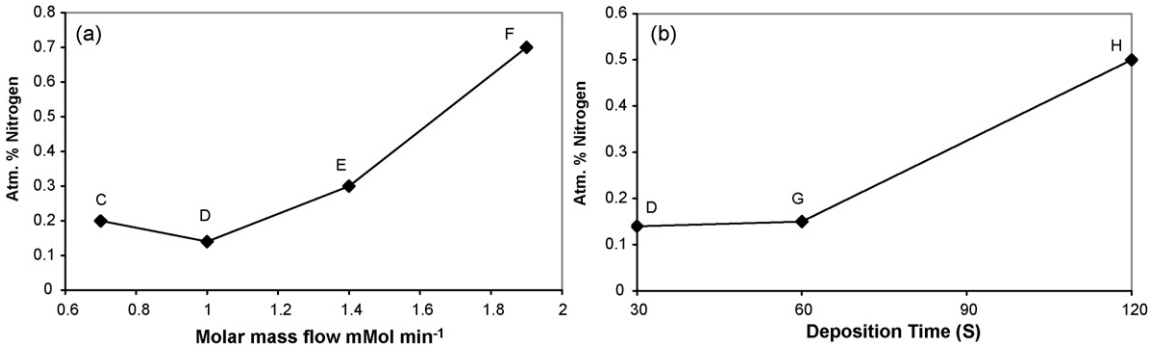

Fig. 8. (a) Schematic showing how the nitrogen content of the different preparations changes with t-butylamine molar gas flow. (b) Schematic showing the composition of the nitrogen content of the films with respect to deposition time. Graphs were derived from the XPS data for the films formed from the APCVD of titanium (IV) chloride, ethyl acetate and t-butylamine at 500 °C. Samples **C**, **D**, **E** and **F** had a 30 s deposition times with increasing molar mass flow of t-butylamine, while **G** and **H** were prepared with a 60 and 120 s deposition time respectively and a molar mass flow for the t-butylamine of 1 mmol min^{-1}.

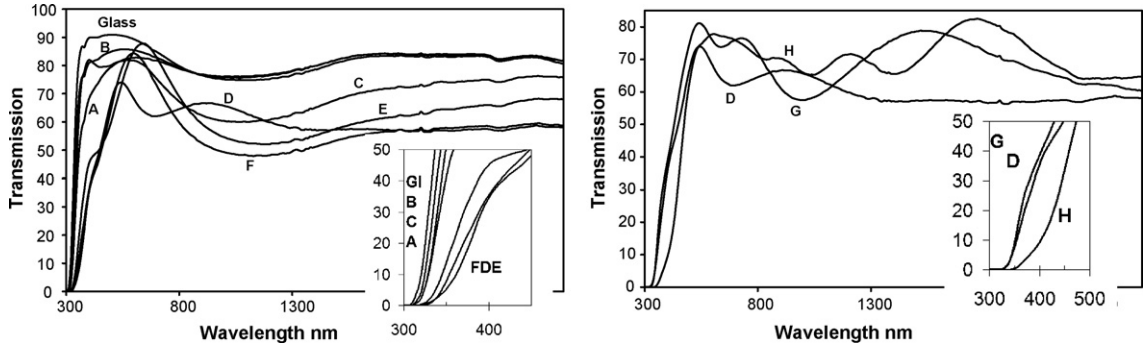

Fig. 9. Transmission data for the full spectrum between 2500 and 300 nm for all the thin films of N-doped TiO_2 formed from APCVD of titanium (IV) chloride, ethyl acetate and t-butylamine prepared at 500 °C and a glass standard. Samples **A** and **B** are Activ™ and BIOCLEAN™ respectively with **GI** indicating the plain glass sample. Samples **C**, **D**, **E** and **F** were prepared with a molar mass flow of for the t-butylamine at 0.7, 1, 1.4 and 1.9 mmol min^{-1} respectively and 30 s deposition times while **G** and **H** were prepared with a 60 and 120 s deposition time respectively and a molar mass flow for the t-butylamine of 1 mmol min^{-1}.

same band onset at 2.75 eV while the 120 s deposition time has a lower band onset at about 2.6 eV. This film does have a significant rutile contribution which will lead to some shifting of the band onset however not as far as the 2.6 eV observed. There is therefore some contribution to the shifting band onset from the nitrogen dopant, though it is unclear whether the dopant is having this effect on the rutile or the anatase structure as both are present.

The films of all samples consisted of nano-particulates of varying size, ranging from 100 to 200 nm (Fig. 11) when analysed by SEM. The size appears to relate to the nitrogen content with all the films prepared with a t-butylamine mass flow rate of 1 mmol min^{-1} (**D**, **G** and **H**) having very similar particle sizes. Sample **F**, prepared with a 1.9 mmol min^{-1} mass flow of t-butylamine also showed comparable particle sizes with that of the afore mentioned preparations. The other preparations show a slightly decreased particle size. The images were analysed using Image-J software [34] with 20 random representative particles measured and the average diameter calculated. Samples **D**, **G** and **H** showed average particle sizes ~186, ~190 and ~150 nm respectively while **C**, **E** and **F** showed particles of average size ~115 nm. This has an affect on the photoactivity of the surfaces [19]. No chlorine impurities were observed using EDX indicating that contamination form the chloride precursor did not occur during the CVD reaction.

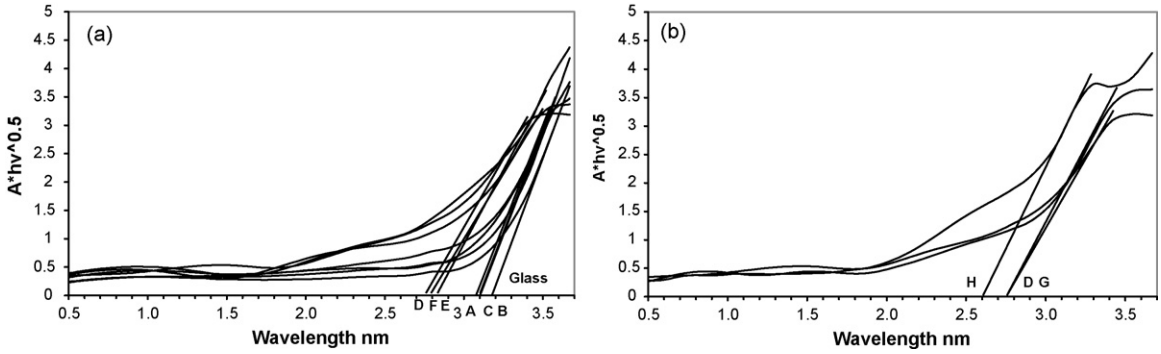

Fig. 10. Tauc plots estimating the band onset for the different films. (a) showing the variation with mass flow of t-butylamine and (b) showing the variation with deposition time. Samples **A** and **B** are Active™ and BIOCLEAN™, samples **C**, **D**, **E** and **F** were prepared with a molar mass flow of for the t-butylamine at 0.7, 1, 1.4 and 1.9 mmol min^{-1} respectively and 30 s deposition times while samples **G** and **H** were prepared with a 60 and 120 s deposition time respectively and a molar mass flow for the t-butylamine of 1 mmol min^{-1}.

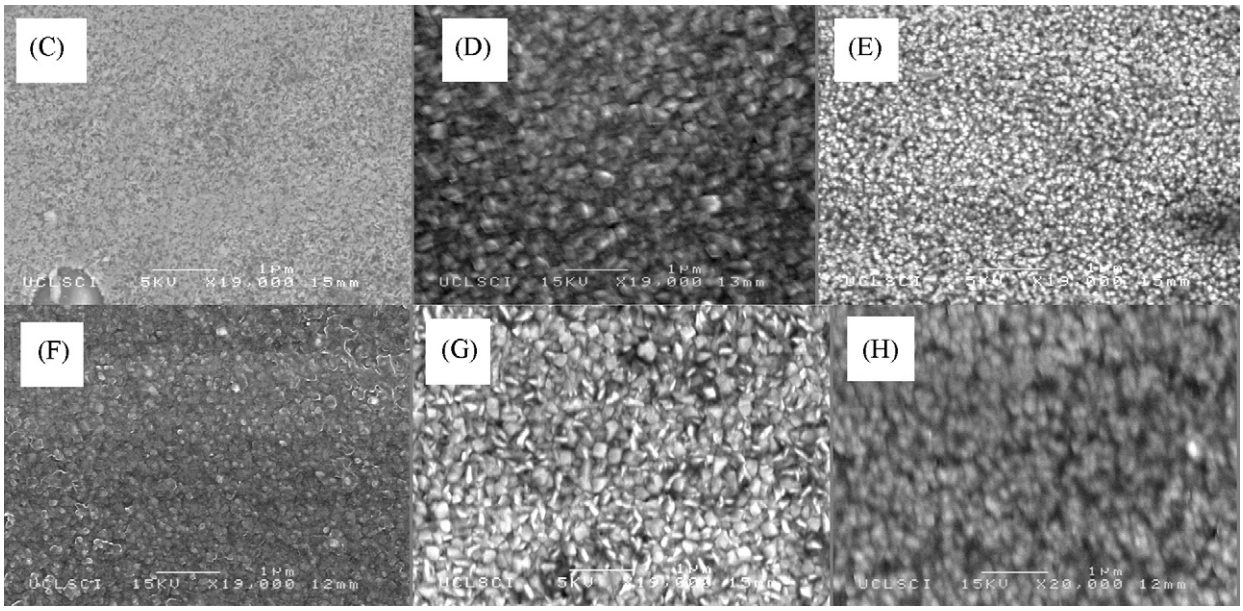

Fig. 11. SEM micrographs of the films of N-doped TiO_2 formed from APCVD of titanium (IV) chloride, ethyl acetate and t-butylamine at 500 °C showing the nano-particulate nature of the thin films and the difference in size of the particulates in each case. Samples **C**, **D**, **E** and **F** were prepared with a molar mass flow of for the t-butylamine at 0.7, 1, 1.4 and 1.9 mmol min^{-1} respectively and 30 s deposition times while **G** and **H** were prepared with a 60 and 120 s deposition time respectively and a molar mass flow for the t-butylamine of 1 mmol min^{-1}.

3.2. Functional testing—hydrophilicity and photocatalysis

Water contact angle measurements were performed by measuring the diameter of a 5 μl drop of deionised water placed on the surface of the film. Measurements were taken before and after activation. The samples were placed in a black box for 72 h prior to the initial reading to fully deactivate the surface and then irradiated by UV light (245 nm) to obtain a maximum value for the hydrophilicity of the surface. Irradiation of the samples under visible light had a similar effect on the contact angles with visible light active samples **C**–**H** but not on the samples requiring UV light for activation **A** and **B** as the superhydrophilicity arises as a consequence of the removal of organic species from the surface due to the photocatalytic activity [35]. The irradiation time was however significantly longer. The results from the UV irradiation are given in Table 2 and show that after UV irradiation all samples are superhydrophilic (contact angle < 10°) with only a small spread between samples. The incorporation of the nitrogen has slightly improved the superhydrophilicity of the surface (3–8°) with respect to Activ™ and BIOCLEAN™ (12–14°) which is a beneficial property of self-cleaning technologies. There is a slight variation between these samples (3–8°), however all are superhydrophilic and comparably better than Activ™ and BIOCLEAN™.

The photocatalysis of the samples was determined by the stearic acid test, whereby a thin layer of stearic acid was applied to the surface in methanol, allowed to evaporate and the decrease in the C–H stretching bands quantified with irradiation time. Fig. 12 shows an appreciable decrease in concentration of stearic acid for the N-doped samples with respect to that observed for Activ™ and BIOCLEAN™ under visible light, with no UV component (no measured emission below 400 nm). Despite these conditions Activ™ did show a small reduction in stearic acid concentration (ca. 10%). There is no apparent trend in position of the stearic acid concentration after prolonged irradiation for the films prepared with a 30 s deposition time (**C**–**F**). The three samples with a t-butylamine mass flow rate of 1 mmol min^{-1} (**D**, **G** and **H**) did however show enhanced reduction in stearic acid concentration with respect to all the other samples. IR spectra before the application of stearic acid showed no C–H stretches indicating that the entirety of the peak was due to the stearic acid and that there was no hydrocarbon contamination in the films from the deposition mixture.

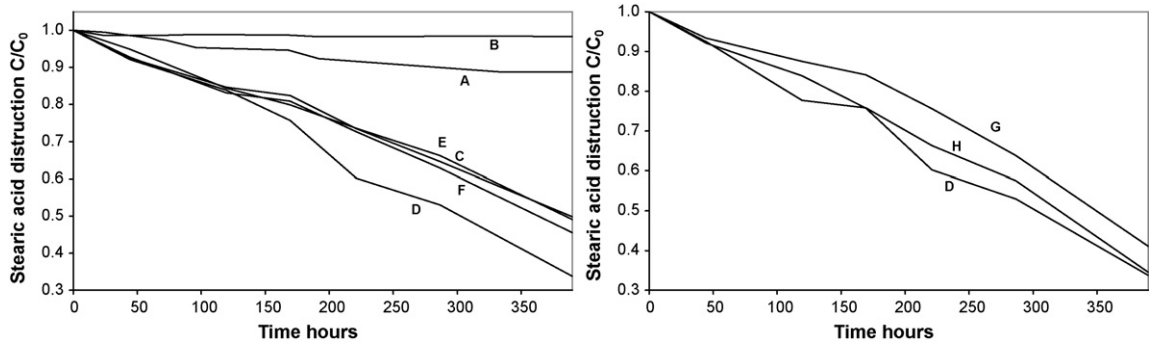

Fig. 12. Results showing the normalised destruction of stearic acid with respect to time for the eight different films of N-doped TiO_2 formed from APCVD of titanium (IV) chloride, ethyl acetate and t-butylamine at 500 °C, irradiated using visible light. Samples **A** and **B** were Active™ and BIOCLEAN™ **C**, **D**, **E** and **F** were prepared with a molar mass flow of for the t-butylamine at 0.7, 1, 1.4 and 1.9 mmol min^{-1} respectively and 30 s deposition times while **G** and **H** were prepared with a 60 and 120 s deposition time respectively and a molar mass flow for the t-butylamine of 1 mmol min^{-1}.

Table 2
The contact angle measurements for the different films of N-doped TiO_2 formed from APCVD of titanium (IV) chloride, ethyl acetate and t-butylamine at 500 °C and the untreated Glass substrate. The samples were stored in a dark container for 4 days prior to testing for the "Before" measurement. The "After" measurements occurred after 24 h activation by 254 nm radiation. Sample **A** was Activ™, sample **B** was BIOCLEAN™, **C**, **D**, **E** and **F** were prepared with a molar mass flow of for the t-butylamine at 0.7, 1, 1.4 and 1.9 mmol min^{-1} respectively and 30 s deposition times while **G** and **H** were prepared with a 60 and 120 s deposition time respectively and a molar mass flow for the t-butylamine of 1 mmol min^{-1}.

Sample	Before	After
Glass	70°	70°
A	60°	12°
B	76°	14°
C	31°	4°
D	86°	5°
E	85°	4°
F	84°	8°
G	72°	8°
H	76°	3°

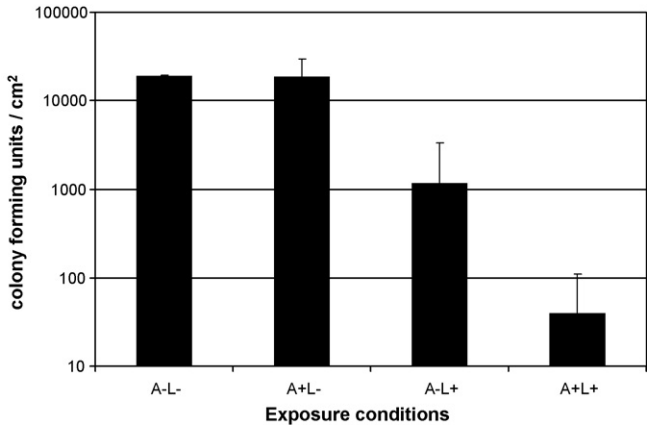

Fig. 13. Survival of *E. coli* on sample **D** after exposure to the white light source. Samples were either exposed to two 24-h light doses (A+L+), an activating 24 h white light dose before the addition of *E. coli* (A+L−), 24 h white light irradiation after *E. coli* addition (A−L+) or incubated in the absence of light throughout (A−L−). Bars indicate median values from the data sets. A+L+ shows a 2.8 log kill (99.9%) while A−L+ shows a 1.2 log kill (99.4%) compared with the A−L− control.

The sample prepared at a flow rate of 1 mmol min^{-1} (sample **D**) showed the most promise for use as a visible light photocatalysis and was therefore used for the microbiology testing. The survival of *E. coli* is illustrated in Fig. 13. When the coatings were activated under white light conditions typically used in UK hospitals for 24 h and then re-incubated with *E. coli* under the same light source for a further 24 h (A+L+), 99.9% of *E. coli* was killed, compared with the A−L− control incubated in the absence of light ($p = 0.01$). Exposing the coatings to just the second light condition resulted in a 94.1% kill ($p = 0.03$), which was also statistically significant. Exposing the coatings to the initial activating light dose only (A+L−) did not have a significant killing effect on *E. coli* ($p = 0.68$). Therefore, an additive effect was observed whereby exposure to either the second light dose or both light doses resulted in a significant kill, with the greatest reduction in bacteria observed after both light exposure periods.

4. Discussion

The use of t-butylamine as a nitrogen source has advantages over using ammonia directly as it prevents the pre-reaction of the components prior to deposition on the desired surface. It is likely that the nitridation occurs as a result of *in situ* ammonia formation as the t-butylamine can thermally decompose into ammonia and isobutylene (Fig. 4) [36,37]. At 500 °C on the substrate, the rate of decomposition of the t-butylamine will be fast in relation to the time that the decomposition mixture of gasses remains in the reaction chamber. The isobutylene has no further reaction under the conditions used and exits via the exhaust [38]. Similar experiments on the same apparatus using ammonia as the nitrogen source failed to yield suitable N-doped TiO_2 films and were highly susceptible to pre-reaction and control-line blockages. The use of t-butylamine has been shown to reduce blockages, reduce gas phase nucleation and associated pin-hole defects. Industrially titanium (IV) chloride and ethyl acetate are used in the production of self-cleaning glass, hence their use here as precursors. It should be noted however that industrially the method of mixing and transport of the precursors would be very different, e.g. in general mass flow controllers would be used to deliver the reactants and the gas outlets would be stable with the glass sheets moving underneath as they come off the float line at 500–600 °C.

The XRD results for the N-doped coatings reported here from APCVD reactions, correlate with a number of conclusions reported by other authors in that the incorporation of nitrogen at low doping concentrations does appear to inhibit the formation of rutile structure and that anatase is the dominant structure in the films grown at 500 °C [29,39]. Surprisingly however the film deposited over 120 s with the highest nitrogen content of our samples has a significant rutile content and is indeed a mixed phase film comprising of crystalline anatase and rutile structures. Thus it seems in this system that anatase is deposited first, but on increasing film thickness a higher proportion of rutile is observed.

The Raman results mirror those observed by the XRD studies. Other researchers using different synthesis techniques have also shown that the incorporation of nitrogen into the titanium dioxide lattice lowers the crystallinity of the films especially at high dopant concentrations [14,17].

The combination of the XPS and the XRD suggests that the film formed with a 60 s deposition is identical to that from a 30 s deposition in a material context, though the 60 s film is clearly thicker. However, the film deposited over 120 s is different with much more significant rutile phase content. We suspect that it is the nitrogen content that encourages the rutile phase. This is because we have made over 300 films of titania by APCVD at 500 °C of varying thickness, but without exception we have only found anatase and not rutile [29,40].

There is much contention and confusion in the N-doped TiO_2 literature about the relationship between the position of the dopant within the lattice and the photocatalytic properties of the material. This is compounded by the difficulty in comparing films produced under different synthetic conditions [41]. Previous work carried out by Mills et al. has attempted to form a reliable test as a recognized benchmark [28,42–44]. Some N-TiO_2 films are reported to be better photocatalysts and indeed work under visible light, while others are worse. For example Yates et al. made a series of N-doped (β substituted XPS ionisation 396 eV) titania films by CVD that were inferior photocatalysts to titania films [41]. It thus appears that it is not only the quantity of nitrogen that is important [45] but also the position of this nitrogen within the lattice which can be probed using XPS. Thompson and Yates [31] show in their review of the subject, how there are two main arguments. Asahi et al. account for the enhanced photocatalytic activity of N-TiO_2 by way of substitutional doping and an XPS ionisation at 396 eV [23] while Diwald et al. account for enhanced photocatalytic activity by way of interstitial doping and a ionisation at ~400 eV [21,46]. Other scientists appear to be evenly split in favour of the two differing opinions [31], or claim that both Interstitial and substitutional have an effect though the interstitial is more pronounced [27]. There is however general agreement that the ionisation at 400 eV is due to interstitial

doping and the ionisation at 396 eV is due to substitutional doping [21,26,27,30,31,41,46,47].

One of the biggest problems with the confusion of the origin of the photocatalytic activity is the ability to prepare samples, films or powders, of N-TiO_2 which display only one ionisation peak in the XPS. Asahi et al. show in their paper a significant enhancement in the XPS peak at 400 eV when comparing the TiO_2 and N-TiO_2 samples as well as the appearance of the peak at 396 eV [23]. Allowing us to conclude that maybe they are doping both in the substitutional site, as stated, with the ionisation at 396 eV but also in the interstitial holes, with the enhancement of the ionisation at 400 eV. Thus the photocatalytic enhancement could be from interstitial dopants rather than substitutional dopants.

Our research shows that the enhanced photocatalytic properties only display when the N (1s) ionisation at 400 eV in the XPS is evident and therefore interstitial doping is of key importance to visible light photocatalysis in N-TiO_2 doped structures. In previous literature reports into N-doped thin films, either just a 396 eV ionisation or a mixed 396 eV and 400 eV ionisation peaks are reported (e.g. [17,18,20,23,30,41]).

Added confusion arises as selective doping is hard to achieve. Many samples reported in the literature show ionisations at both 396 eV and 400 eV which may have opposite effects that cancel out. The synthetic method of preparation therefore plays a major role in the doping position, i.e. substitutional or interstitial, and as a result is key to the formation of both highly active and visible active photocatalytic films. The quantity of nitrogen doping is also key to the formation of good photocatalytic films as high levels of doping, formed by other methods result in low activity [45]. Typical results show 1–2 at.% is best for powders. Our results (see above) corroborate this, albeit at a lower concentration (0.13–0.7 at.%) with the lowest incorporation of nitrogen just in an interstitial site corresponding to the highest activity.

The use of t-butylamine appears to give the mass flow control required and surface chemistry to achieve interstitial doping. The *in situ* production of ammonia along with isobutylene on the surface of the glass substrate appears to provide good conditions to insert nitrogen atoms into the lattice without removing oxygen atoms, hence achieving interstitial doping rather than substitutional doping and the attributed enhancement in photocatalytic properties. Work by us using ammonia directly as a N-source in making compositional gradient Ti–O–N films shows that the N-doping always occurs in the substitutional (396 eV) form [38].

The stability of interstitial doping of nitrogen raises many questions as there is likely a high degree of nitrogen mobility. Loss of nitrogen would hinder the photocatalytic activity of the film reducing its effectiveness. There is however little evidence from our results that this occurs as the XPS was performed 6 months after some of the samples were prepared and multiple runs using stearic acid show similar results again over a 6-month period. Whether the films remain stable and efficient photocatalysts over a period of decades has yet to be tested.

The exact role of the environment in healthcare-associated infections has yet to be fully elucidated, but it is advantageous to ensure that the microbial population within a hospital setting is kept to a minimum. Antibacterial coatings present a novel approach to preventing the transfer of bacteria from patient to patient and ultimately fighting healthcare-associated infections, and could be used alongside meticulous hand hygiene and prudent antibiotic prescribing policies. The N-doped film prepared with a 30 s deposition time and a mass flow of 1 mmol min^{-1} t-butylamine, sample **D**, is an example of a novel antibacterial coating that is activated by the white light used in many UK hospitals. This preliminary study has shown that this sample when activated was capable of killing 99.9% of an *E. coli* suspension containing more than 10^4 viable bacteria, when exposed to 24 h of white light using typical hospital lighting conditions. This killing effect was not seen when the slides were incubated in the absence of light. These data provide an exciting opportunity to explore these novel compounds further, testing them against a range of pathogenic microorganisms which are found in the hospital environment and presents a solid foundation for future work. It has previously been shown that *E. coli* being a Gram-negative bacterium is far less susceptible to photo-induced destruction than Gram-positive organisms [11] leading to a high reality that the antimicrobial effects should be more enhanced with other bacteria such as Gram-positive MRSA and such like. These coatings therefore provide a potential method for the control and prevention of hospital acquired infections.

5. Conclusions

A series of thin films of N-doped titania have been prepared and characterised. Of the series it was found that the best photocatalytic properties were obtained from the films prepared with a flow rate of 1 mmol min^{-1} of t-butylamine as a reacting precursor. It has been shown that interstitial nitrogen doping (XPS ionisation at 400 eV) of the anatase structure of titania is preferable to substitutional doping (XPS ionisation at 396 eV) if visible light photocatalytic properties are desired. This is the first preparation of a photocatalytically enhanced film to show only the 400 eV and not the 396 eV XPS ionisations.

The use of titanium (IV) chloride, ethyl acetate and t-butylamine provide a clean and direct route to enhanced photocatalysts in a methodology that is entirely compatible with current float glass industrial practices leading to high potential for swift incorporation and movement from first generation to second generation self-cleaning windows. To our knowledge this is the first known example of antimicrobial property displayed for N-doped titania films showing a 99.9% kill of *E-coli* under conditions typically observed in UK hospitals.

Acknowledgements

The authors thank the EPSRC for financial support. IPP thanks the Royal Society Wolfson trust for a merit award. DJM also thanks the EPSRC for the Access to Research Equipment initiative (grant number EP/F019823/1).

References

[1] http://www.pilkington.com, last accessed in 2009.
[2] A. Mills, G. Hill, M. Crow, S. Hodgen, Journal of Applied Electrochemistry (2005) 641.
[3] http://www.selfcleaningglass.com, last accessed in 2009.
[4] http://www.suncleanglass.com, last accessed in 2009.
[5] A. Mills, N. Elliott, I.P. Parkin, S. O'Neill, R.J.H. Clark, Journal of Photochemistry and Photobiology A: Chemistry 151 (2002) 171.
[6] A. Mills, S. Le Hunte, Journal of Photochemistry and Photobiology A: Chemistry 108 (1997) 1.
[7] S. Noimark, C. Dunnill, M. Wilson, I.P. Parkin, Chemical Society Reviews (2009), doi:10.1039/B908260C.
[8] W. Curdt, P. Brekke, U. Feldman, K. Wilhelm, B.N. Dwivedi, U. Schuhle, P. Lemaire, Solar and Galactic Composition 598 (2001) 45.
[9] Health Protection Agency Commission of the European Communities, 2005. http://eur-lex.europa.eu/LexUriServ/LexUriServ.do?uri=CELEX:32005R2073:EN:NOT.
[10] R.M. Klevens, J.R. Edwards, C.L.J. Richards, T.C. Horan, R.P. Gaynes, D.A. Pollock, D.M. Cardo, Public Health Reports 122 (*2*) (2007) 160.
[11] V. Decraene, J. Pratten, M. Wilson, Applied and Environmental Microbiology 72 (2006) 4436.
[12] Y. Guo, X.-W. Zhang, W.-H. Weng, G.-R. Han, Thin Solid Films 515 (2007) 7117.
[13] M. Masahiko, W. Teruyoshi, Journal of the Electrochemical Society 153 (2006) C186.
[14] F.D. Duminica, F. Maury, R. Hausbrand, Surface and Coatings Technology 201 (2007) 9349.
[15] J. Yang, H. Bai, Q. Jiang, J. Lian, Thin Solid Films 516 (2008) 1736.
[16] K. Yamada, H. Yamane, S. Matsushima, H. Nakamura, T. Sonoda, S. Miura, K. Kumada, Thin Solid Films 516 (2008) 7560.

[17] T. Okato, T. Sakano, M. Obara, Physical Review B 72 (2005) 115124.
[18] C. Hsyi-En, L. Wen-Jen, H. Ching-Ming, H. Ming-Hsiung, H. Chien-Lung, Electrochemical and Solid-State Letters 11 (2008) D81.
[19] Y. Guo, X.-W. Zhang, G.-R. Han, Materials Science and Engineering B 135 (2006) 83.
[20] M. Gartner, P. Osiceanu, M. Anastasescu, T. Stoica, T.F. Stoica, C. Trapalis, T. Giannakopoulou, N. Todorova, A. Lagoyannis, Thin Solid Films 516 (2008) 8184.
[21] O. Diwald, T.L. Thompson, T. Zubkov, E.G. Goralski, S.D. Walck, J.T. Yates, The Journal of Physical Chemistry B 108 (2004) 6004.
[22] O. Diwald, T.L. Thompson, E.G. Goralski, S.D. Walck, J.T. Yates, The Journal of Physical Chemistry B 108 (2004) 52.
[23] R. Asahi, T. Morikawa, K. Ohwaki, K. Aoki, Y. Taga, Science 293 (2001) 269.
[24] A. Borras, C. Lopez, V. Rico, F. Gracia, A.R. Gonzalez-Elipe, E. Richter, G. Battiston, R. Gerbasi, N. McSporran, G. Sauthier, E. Gyorgy, A. Figueras, The Journal of Physical Chemistry C 111 (2007) 1801.
[25] L.K. Randeniya, A. Bendavid, P.J. Martin, E.W. Preston, The Journal of Physical Chemistry C 111 (2007) 18334.
[26] A.V. Emeline, V.N. Kuznetsov, V.K. Rybchuk, N. Serpone, International journal of photoenergy 2008 (2008) 258394.
[27] F. Peng, L. Cai, H. Yu, H. Wang, J. Yang, Journal of Solid State Chemistry 181 (2008) 130.
[28] A. Mills, J. Wang, Journal of Photochemistry and Photobiology A: Chemistry 182 (2006) 181.
[29] G. Hyett, M. Green, I.P. Parkin, Journal of the American Chemical Society 128 (2006) 12147.
[30] N.C. Saha, G.H. Tompkins, Journal of Applied Physics 72 (1992) 3072.
[31] T.L. Thompson, J.T. Yates, Chemical Reviews 106 (2006) 4428.
[32] C. Guimon, A. Gervasini, A. Auroux, The Journal of Physical Chemistry B 105 (2001) 10316.
[33] R. Swanepoel, Journal of Physics E 16 (1983) 1214.
[34] http://rsbweb.nih.gov/ij/, last accessed in 2009.
[35] T. Zubkov, D. Stahl, T.L. Thompson, D. Panayotov, O. Diwald, J.T. Yates, The Journal of Physical Chemistry B 109 (2005) 15454.
[36] H.O. Pritchard, R.G. Sowden, A.F. Trotman-Dickenson, Journal of the Chemical Society (1954) 546.
[37] J.-B. Wu, Y.-W. Yang, Y.-F. Lin, H.-T. Chiu, The Journal of Physical Chemistry B 108 (2004) 1677.
[38] G. Hyett, M.A. Green, I.P. Parkin, Journal of the American Chemical Society 129 (2007) 15541.
[39] T. Lindgren, J.M. Mwabora, E. Avendano, J. Jonsson, A. Hoel, C.G. Granqvist, S.E. Lindquist, The Journal of Physical Chemistry B 107 (2003) 5709.
[40] I.P. Parkin, R.G. Palgrave, Journal of Materials Chemistry 15 (2005) 1689.
[41] H.M. Yates, M.G. Nolan, D.W. Sheel, M.E. Pemble, Journal of Photochemistry and Photobiology A: Chemistry 179 (2006) 213.
[42] A. Mills, M. McFarlane, Catalysis Today 129 (2007) 22.
[43] A. Mills, M. McGrady, J. Photochemistry and Photobiology A: Chemistry 193 (2008) 228.
[44] A. Mills, J. Wang, S.-K. Lee, M. Simonsen, Chemical Communications (2005) 2721.
[45] H. Irie, Y. Watanabe, K. Hashimoto, The Journal of Physical Chemistry B 107 (2003) 5483.
[46] C. Di Valentin, E. Finazzi, G. Pacchioni, A. Selloni, S. Livraghi, M.C. Paganini, E. Giamello, Chemical Physics 339 (2007) 44.
[47] C. Di Valentin, G. Pacchioni, A. Selloni, Physical Review B 70 (2004) 085116.
[48] http://www.gelighting.com/eu/resources/literature_library/prod_tech_pub/downloads/biax2d_datasheet_0506.pdf, last accessed in 2009.